Australian Earthquake Engineering Society
National Conference, 20-22 November 2025
Melbourne, Victoria

Are ground motions in Australia different between cratonic and non-cratonic regions, and different from global models?

Jeff Bayless[1] and Paul Somerville[2]

1. AECOM, Los Angeles, jeff.bayless@aecom.com
2. AECOM, Los Angeles, paul.somerville@aecom.com

Abstract

The objective of this paper is to address two questions about ground motion models (GMMs) in Australia. Firstly, in what ways do ground motions from non-cratonic earthquakes differ from those of cratonic earthquakes in Australia? To explore this question, we used ground motions and stress drops from cratonic and non-cratonic Australian earthquakes. We compared attenuation and response spectral shapes between the cratonic and non-cratonic events and with a suite of twelve GMMs (including NGA-East; Goulet et al., 2021, NGA-West2; summarised in Gregor et al., 2014, Allen 2012, Drouet 2015, Atkinson and Boore 2006, Somerville et al., 2009, and Bayless and Somerville, 2024). With our GMM residual analysis, we found approximately 10% – 50% higher ground motions on average for the cratonic dataset, and using stress drops from Allen (2025) we found a statistically significant difference in average stress drops for the cratonic and non-cratonic regions. Secondly, are the NGA-East and NGA-West2 GMMs, which were developed for use in eastern North America and in tectonically active regions of the world respectively, applicable to seismic hazard studies in Australia, and if so, in which regions of Australia? This was investigated by comparing the magnitude and distance scaling of the GMMs in the ranges often critical for seismic hazard. The benefit of using the NGA models is that they are calibrated for large magnitudes and short distances, which cannot be done empirically in Australia. Because of the great care that went into the scaling of the NGA models, particularly in magnitude and distance ranges where we do not have data in Australia, we consider these models applicable to Australia.

Keywords: ground motion models, cratonic, non-cratonic.

1 Introduction

Ground motion models (GMMs) estimate the ground motion and its variability as a function of the distance from causative fault, earthquake magnitude, seismic wave attenuation from source to site, near-surface ground conditions (e.g., V_{S30}) and other seismological or geotechnical parameters. GMMs are commonly developed for different tectonic regimes and are usually developed by fitting seismological models to data collected by strong-motion instruments from earthquakes globally, regionally, or if there are enough data available, to site-specific earthquake ground motion data. GMMs underpin the seismic hazard results and drive the design ground motions in future engineering guidelines and for infrastructure projects.

Geoscience Australia's 2023 National Seismic Hazard Assessment (NSHA23; Allen et al, 2023; 2024) points out that there is a relative paucity of data from which to develop empirical GMMs in Australia, and that this contributes significantly to the total uncertainty in the probabilistic seismic hazard analyses (PSHAs). To address this, NSHA23 considered Australian-specific GMMs in addition to models developed outside Australia, using an updated

suite of ground motion data from small-to-moderate magnitude Australian earthquakes (Ghasemi and Allen, 2021, 2023) to empirically assess the suitability of the candidate models. These analyses used a relatively limited set of data - much less than we now have available. The candidate models along with the qualitative and quantitative measures of this study were presented in an expert elicitation workshop to support data driven selection and ranking of GMMs for the NSHA23 (Allen et al., 2023). In the end, NSHA23 did not use any high-attenuation GMMs developed for active tectonic regions (e.g., those from NGA-West2).

In this paper, with the aim of improving future ground motion characterisation models for seismic hazard studies in Australia, we supplement the NSHA23 evaluation of candidate GMMs with a focus on two questions:

(1) In what ways, if any, do ground motions from non-cratonic earthquakes differ from those of cratonic earthquakes in Australia?

(2) Are the NGA-East (Goulet et al., 2021) and NGA-West2 (summarised in Gregor et al., 2014) ground motion models, which were developed for use in eastern North America and in tectonically active regions of the world respectively, applicable in Australia, and if so, in which regions of Australia?

The NSHA23 used a simplified mapping of tectonic regions to three ground motion model logic trees: Cratonic, Non-cratonic, and Subduction, where shallow active crustal sources from the northern plate margin source model (Griffin and Davies, 2018), extended, and oceanic crustal tectonic regions were mapped to non-cratonic regions (Figure 1).

For addressing the two research questions of this paper, we used the twelve GMMs listed in Table 1. All the GMMs listed in Table 1 are for the horizontal component (RotD50 or geometric mean) of 5% damped spectral acceleration.

2 Recorded Ground Motion Response Spectra

In Bayless and Somerville (2024), we compiled (1) a cratonic earthquake ground motion dataset including waveform data from Geoscience Australia (Ghasemi and Allen, 2021), who provided instrument corrected recordings for events occurring within cratonic regions, and from IRIS (https://ds.iris.edu/wilber3/), and (2) a non-cratonic ground motion dataset of response spectra and metadata, provided by Geoscience Australia (Trevor Allen, personal communication). In the cratonic dataset, there are 33 events with $3.5 \leq \mathbf{M} < 4.0$ and 35 events with $4.0 \leq \mathbf{M} < 5.34$. In the non-cratonic dataset, there are 13 events with $3.6 \leq \mathbf{M} < 5.9$, including the 2021 **M** 5.9 Woods Point and 2012 **M** 5.1 Moe earthquakes. The combined dataset includes 733 records from 98 events, recorded by 313 unique stations with source to site distances up to 600 km. More details about this small-to-moderate magnitude dataset can be found in Bayless and Somerville (2024).

We compared the GMMs in Table 1 with this dataset. For these comparisons, we used a reference site condition of V_{S30} = 760 m/s in the GMMs. The data were adjusted to the V_{S30} = 760 m/s condition using the Seyhan and Stewart (2014) amplification factors for non-cratonic earthquakes and using the linear (gradual velocity gradient model) and non-linear components of Stewart et al. (2020) and Hashash et al. (2020), respectively, for cratonic earthquakes. The uncertainties in V_{S30} values and in the site response adjustments are significant and could be reduced in the future with additional data collection or improved models; these sources of uncertainty were similarly identified and accepted in NGA-East (Goulet et al., 2021).

We compared the distance attenuation (e.g., Figure 2) and response spectral shapes (e.g., Figure 3) for all events in the dataset with the median GMMs listed in Table 1. For the NGA-East model, the weighted mean of the suite of 17 median models was used.

Model Name*	Tectonic Region Type	Intra-Region Weight	Reference
Allen2012_SS14	Non-cratonic, Extended, Oceanic and Active Crust	0.29	Allen (2012)
AtkinsonBoore2006		0.15	Atkinson and Boore (2006)
DrouetBrazil2015		0.17	Drouet (2015)
SomervilleEtAl2009NonCratonic		0.29	Somerville et al. (2009)
NGAEastGMPE		0.10	Goulet et al. (2017)
Allen2012_SS14	Cratonic	0.24	Allen (2012)
AtkinsonBoore2006		0.13	Atkinson and Boore (2006)
DrouetBrazil2015		0.14	Drouet (2015)
ESHM20Craton		0.10	Weatherill et al. (2020)
NGAEastGMPE		0.09	Goulet et al. (2017)
SomervilleEtAl2009YilgarnCraton		0.16	Somerville et al. (2009)
SomervilleEtAl2009NonCratonic		0.14	Somerville et al. (2009)

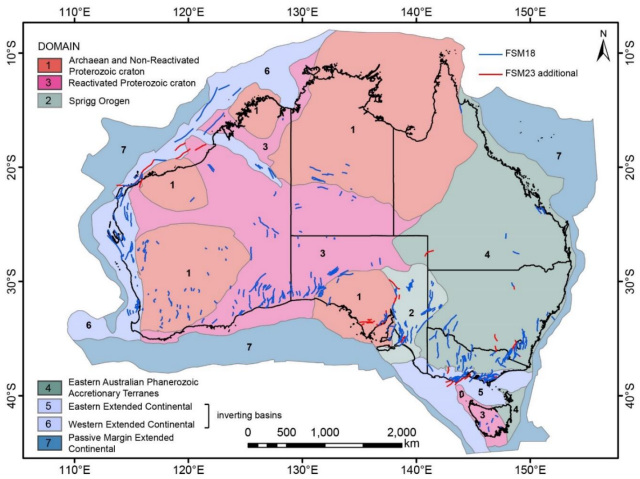

Figure 1. Left: The NSHA23 GMM logic tree for Cratonic and Non-cratonic (Extended, Oceanic, and Active Crust) tectonic regions determined through structured expert elicitation. Right: The neotectonic domains model of Clark et al. (2012) coloured to emphasise cratonic (pale red to pink polygons), Phanerozoic non-extended (green polygons) and extended (blue polygons) domains. Figure source: Allen et al. (2023).

Table 1. The GMMs evaluated in this study.

Model Abbreviation	Reference	Description	Used in NSHA23 Cratonic	Used in NSHA23 Non-cratonic
BS24 Cratonic	Bayless and Somerville (2024)	Update of Sea09; Australia-specific model developed using ground motion simulations and empirical data; cratonic version.	No (developed after NSHA23)	No
BS24 NonCratonic	Bayless and Somerville (2024)	The non-cratonic version of the above.	No	No
Allen12	Allen (2012)	Australia-specific model developed using stochastic method finite fault simulations and validated with earthquakes from eastern Australia.	Yes	Yes
Sea09 Cratonic	Somerville et al. (2009)	Australia-specific model developed using broadband finite fault simulations and validated with Australian earthquake data; cratonic version.	Yes	No
Sea09 NonCratonic	Somerville et al. (2009)	The non-cratonic version of the above.	Yes	Yes
Drouet15	Drouet & Cotton (2015)	Unpublished model for Brazil based on the method described in Drouet & Cotton (2015).	Yes	Yes
AB06	Atkinson and Boore (2006)	Eastern North America model developed using stochastic method finite fault simulations.	Yes	Yes
NGA-East	Goulet et al. (2021)	A suite of 17 models for the Central and Eastern United States, a stable continental region.	Yes	Yes
BSSA14	Boore et al. (2014)	NGA-West2 project model; for shallow crustal earthquakes in tectonically active regions.	No	No
ASK14	Abrahamson et al. (2014)	NGA-West2 project model; for shallow crustal earthquakes in tectonically active regions.	No	No
CY14	Chiou and Youngs (2014)	NGA-West2 project model; for shallow crustal earthquakes in tectonically active regions.	No	No
CB14	Campbell and Bozorgnia (2014)	NGA-West2 project model; for shallow crustal earthquakes in tectonically active regions.	No	No

From the events for which we have the most data at close distances, Moe (**M** 5.10) and Marble Bar (**M** 5.32) have about the same magnitudes and are not shallow earthquakes. Unfortunately, their source-to-site distances do not overlap much, as shown in Figure 2, making it difficult to draw meaningful conclusions about differences between cratonic and non-cratonic distance attenuation from these events. Nonetheless, the scaling of the median GMMs is informative. In general, the suite of median models captures the median of the data in Figure 2. This figure also shows the differences in distance scaling between models, including the Allen12 and AB06 models with a transition zone between approximately 80-150 km in which the ground motions do not decrease with distance, designed to account for direct waves joined by postcritical reflections from the Moho. The other 10 GMMs do not explicitly model this feature. Figure 2 also shows that models based on the R_{jb} distance metric (Drouet15, BSSA14, Sea09) exhibit a curvature at short distances when plotted versus R_{rup}. This is the increase in ground motions due to the parameter R_{jb} approaching zero as R_{rup} approaches the earthquake depth to top of coseismic rupture (Z_{tor}). In the absence of finite fault rupture models and because of the small magnitudes in the dataset, we assumed the earthquake hypocentral depth as equal to Z_{tor}. Finally, the large scatter of the data in Figure 2 demonstrates the significant aleatory variability in the ground motion data.

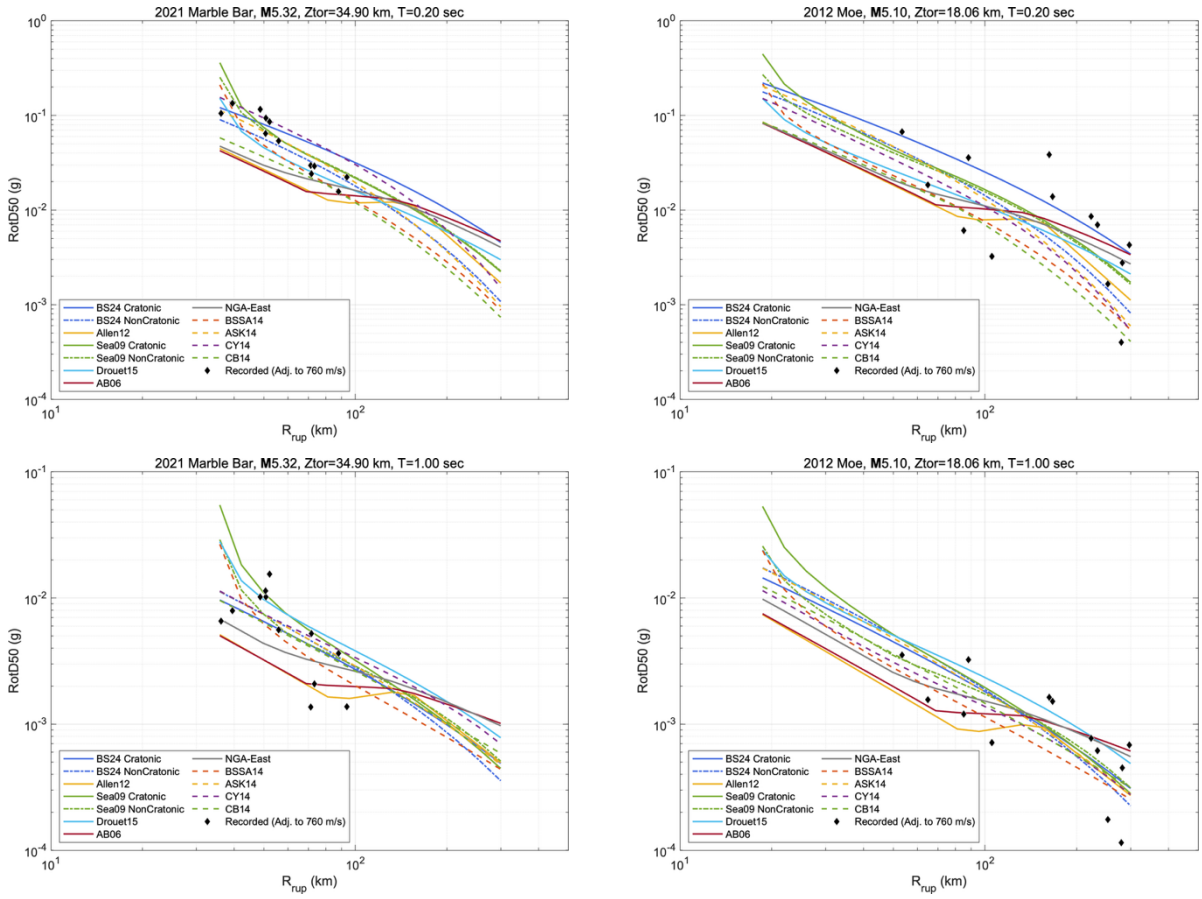

Figure 2. Spectral acceleration (T=0.2 sec, top row; T=1.0 sec, bottom row) with distance for the 2021 Marble Bar earthquake in the Pilbara Craton (left column) and the non-cratonic 2012 Moe earthquake in Victoria (right column), compared with the suite of median GMMs.

Figure 3 compares example recorded response spectra from the Marble Bar (left) and Moe (right) earthquakes, both at about 60-70 km distance. Both recordings show elevated short period (T < 0.1 sec) response spectra that are more consistent with the medians of three stable region models (BS24-Cratonic, Sea09-Cratonic, and NGA-East) and with the CY14 model for the Marble Bar recording. For CY14, this model has been applied outside the largest

recommended Z_{tor} value of 20 km (Marble Bar Z_{tor} = 34.9 km) and this is the cause of the high short period ground motions for this model. At spectral periods longer than about T = 1 sec, the scatter in the median GMMs is reduced relative to shorter periods and the suite of models generally agree with the recordings.

Figure 4 compares the T=0.03 sec distance attenuation for two Northern Territory earthquakes with similar magnitudes and depths, showing short period spectral accelerations consistent with our cratonic model and other stable continental region models, and inconsistent with NGA-West2 models beyond 100 km distance. These relatively shallow earthquakes have smaller physically possible values of R_{rup} and R_{jb} than the deeper earthquakes of Figure 2. This allows for inspection of the distance scaling of the GMMs to very small distances even though no data are available at such distances. Figure 4 shows that for a **M** 5 earthquake at very small distances (R_{rup} < 10 km) the range of median GMMs is about a factor of ten.

Any conclusions drawn from comparisons like Figures 2 through 4 are inherently subjective. In order to provide a more quantitative approach, we performed the GMM residual analyses described in Section 3.

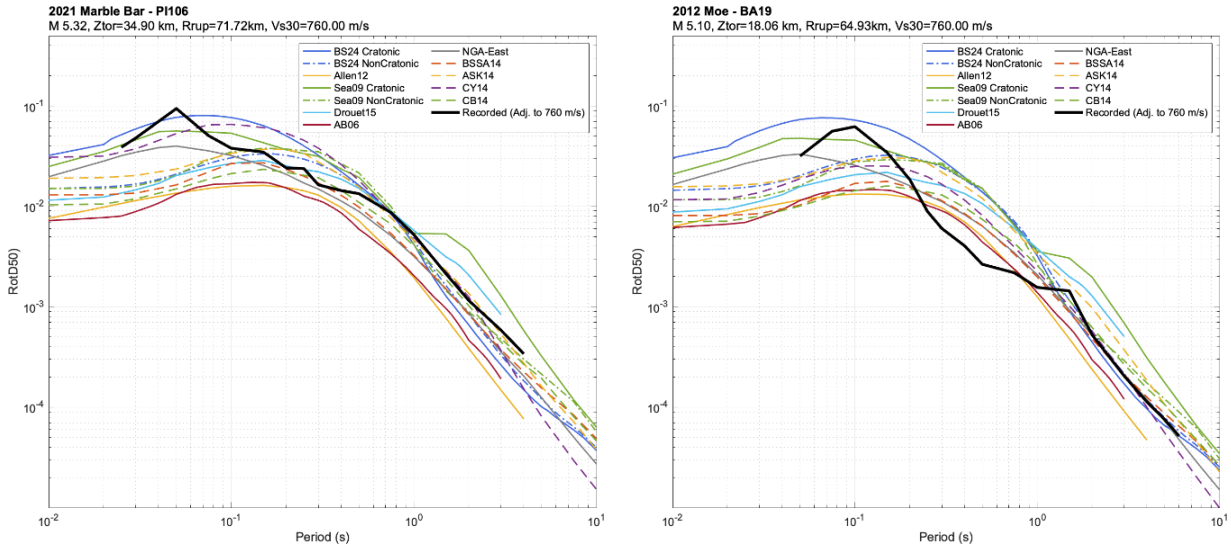

Figure 3. Response spectra recorded in the 2021 Marble Bar earthquake in the Pilbara Craton (left) and the non-cratonic 2012 Moe earthquake in Victoria (right), compared with the suite of median GMMs.

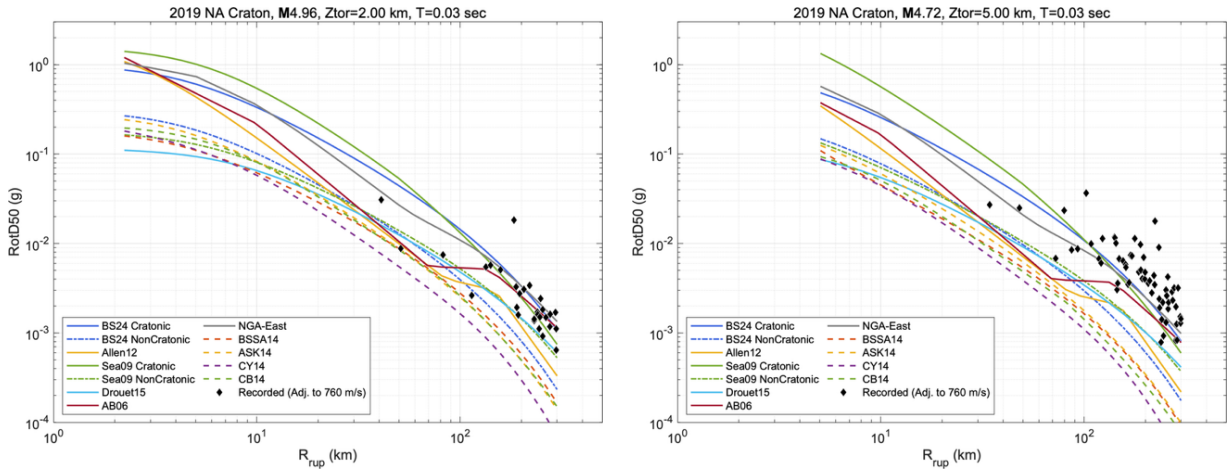

Figure 4. Spectral acceleration (T=0.03 sec) with distance for two Northern Territory earthquakes showing short period accelerations consistent with our cratonic model and other stable continental region models, and inconsistent with NGA-West2 models beyond 100 km distance.

3 GMM Residuals

For each GMM listed in Table 1, we performed a mixed effects regression using the combined cratonic and non-cratonic datasets (minimum 5 recordings per event) adjusted to the V_{S30} = 760 m/s condition as described above. In the regression, the total residual at a given spectral period is defined as the difference between the natural logarithm of the recorded spectral acceleration adjusted to the V_{S30} = 760 m/s condition (data) and the natural logarithm of the median GMM with the same V_{S30} condition. We used a mixed-effects analysis to separate the total residuals into the mean bias term (c_k), the between-event residuals (δB_e) and within-event residuals (δWE_{es}). The data were partitioned to obtain separate mean bias terms for the cratonic ($c_{k,crat}$) and non-cratonic ($c_{k,noncrat}$) datasets. With this approach, the c_k are the mean biases (ln units) of the residuals for the cratonic and non-cratonic datasets, and δB_e and δWE_{es} are well-represented as zero mean, independent, normally distributed random variables with standard deviations τ and ϕ, respectively (Al Atik et al., 2010). The regression was performed for five spectral periods: 0.03, 0.1, 0.3, 1, and 3 sec.

For a given spectral period and GMM, positive values of c_k represent GMM under-prediction on average, and negative values of c_k represent GMM over-prediction on average. The values of c_k for the cratonic and non-cratonic regions are useful indicators for the differences in average ground motions between regions; these are discussed further below.

The δB_e and δWE_{es} residuals are best used to identify trends with the model parameters: **M**, R_{rup}, Z_{tor}, V_{S30}. We reviewed the values of c_k, δB_e and δWE_{es} with these parameters and with spectral period for each GMM, e.g., Figure 5 for the BS24-Cratonic model.

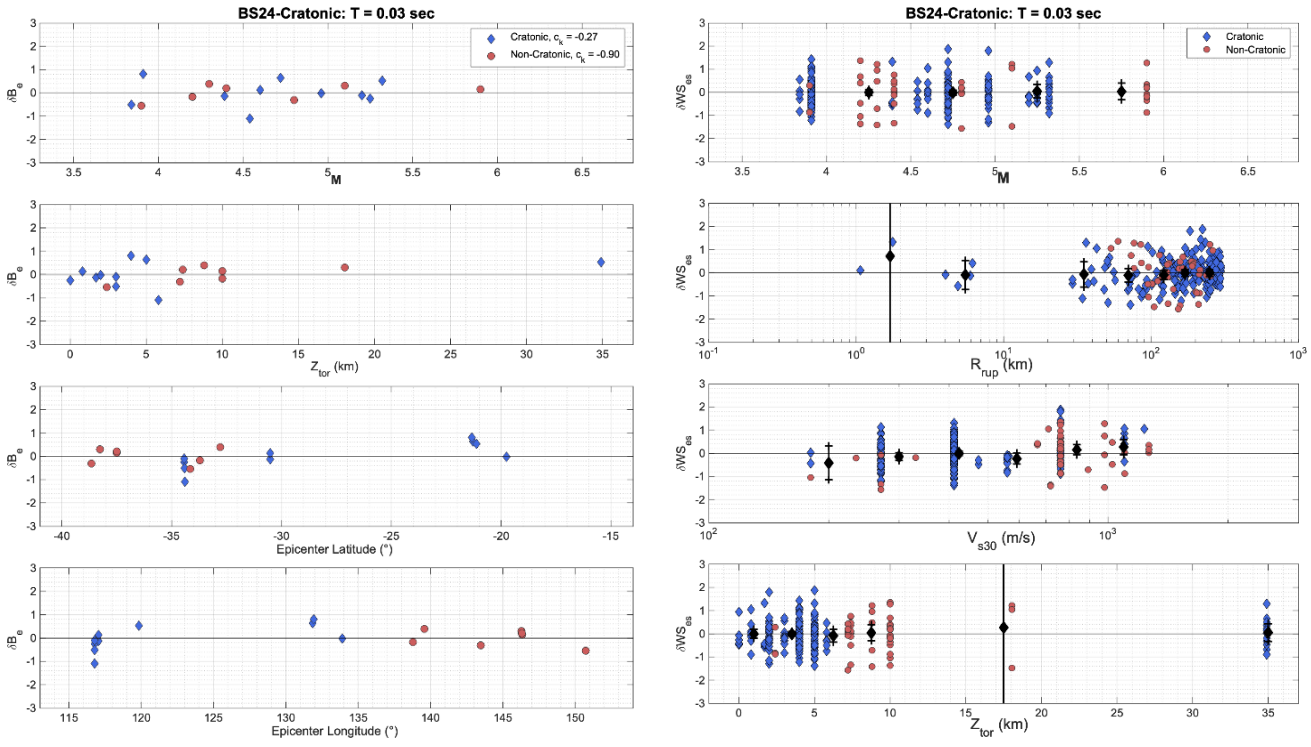

Figure 5. δB_e residuals (left) and δWE_{es} residuals (right) at T=0.03 sec for the BS24-Cratonic model. The values of c_k are shown in the δB_e figure legend. The black diamonds with whiskers represent the mean and 95% confidence interval of the mean for binned ranges of the model parameters.

In summary, we found the following about the δB_e residuals:

- At T = 0.03 sec, fairly weak but observable trends in δB_e with **M** for AB06, Allen12, Drouet, Sea09. Otherwise, no significant trends with **M** or differences in the **M**-scaling between cratonic and non-cratonic datasets.
- At T = 0.03 sec, the very deep (Z_{tor} = 34.9 km) Marble Bar cratonic earthquake has higher δB_e than all other shallower cratonic earthquakes in all models except BS24, Sea09, and the four NGA-West2 models.
- Otherwise, we generally did not find obvious features or strong trends in δB_e with earthquake depth, latitude, or longitude.

And for the δWE_{es} residuals:

- These residuals are most useful for evaluating trends with R_{rup} and V_{S30} because the other parameters (**M**, Z_{tor}, and location) are event-specific and therefore captured in δB_e.
- For most GMMs and at V_{S30} values smaller than 400 m/s, the δWE_{es} are biased low for T < 1 sec, indicating that the V_{s30} scaling models are over-amplifying ground motions for sites with low V_{S30} in this period range. This conclusion is subject to the limitations about our uncertainties in V_{S30} values and site amplification models discussed previously.
- Several GMMs, including all four NGA-West2 models, over-predict the ground motions on average (negative δWE_{es}) in the approximate distance range 50-150 km and under-predict on average in the approximate distance range 150-300 km. The two models with piecewise distance scaling with a transition zone (Allen12 and AB06) appear to best capture the distance scaling in the dataset.

The values of c_k in natural log units (plus and minus one standard error) for the cratonic and non-cratonic regions are shown for each of five spectral periods and for each GMM in Figure 6. Using c_k to compare the differences in ground motions between the cratonic and non-cratonic Australia, we observed the following:

- At T = 0.03, 0.1, and 3 sec, all twelve GMMs have higher c_k for the cratonic dataset than the non-cratonic dataset, showing that the cratonic ground motions are systematically larger than the non-cratonic ground motions on average for these spectral periods.
- At T = 0.3 and T = 1 sec, the difference in c_k between the cratonic and non-cratonic datasets is relatively small compared with the other spectral periods.
- At T = 1 sec, there is best GMM performance overall across models.
- The four NGA-West2 GMMs all under-estimate the short period ground motions on average by substantial factors of 3-4. This bias reduces with increasing spectral period and is likely a combination of both magnitude and distance scaling.

We took the difference in c_k between regions ($\Delta c_k = c_{k,crat} - c_{k,noncrat}$) and calculated the mean of Δc_k across the five spectral periods ($\overline{\Delta c_k}$). For the 12 GMMs, the minimum $\overline{\Delta c_k}$ is 0.10, the maximum is 0.45, and the mean is 0.32 ln units, representing a range of approximately 10% – 50% higher ground motions for the cratonic dataset.

The regression standard deviations of δB_e and δWE_{es}, τ and ϕ respectively, are shown for T = 0.03 sec in Figure 7. At this spectral period, the values of ϕ are systematically larger for the non-cratonic dataset. This difference reduces at other spectral periods and is reversed for T = 1 sec (not shown). The values of τ at T = 0.03 sec are comparable between regions for about half of the GMMs, and larger from the cratonic dataset for the remaining GMMs. For reference, the Al Atik (2015) global aleatory variability model values are τ = 0.43 and ϕ = 0.72 natural log units (**M** 5 and T = 0.03 sec).

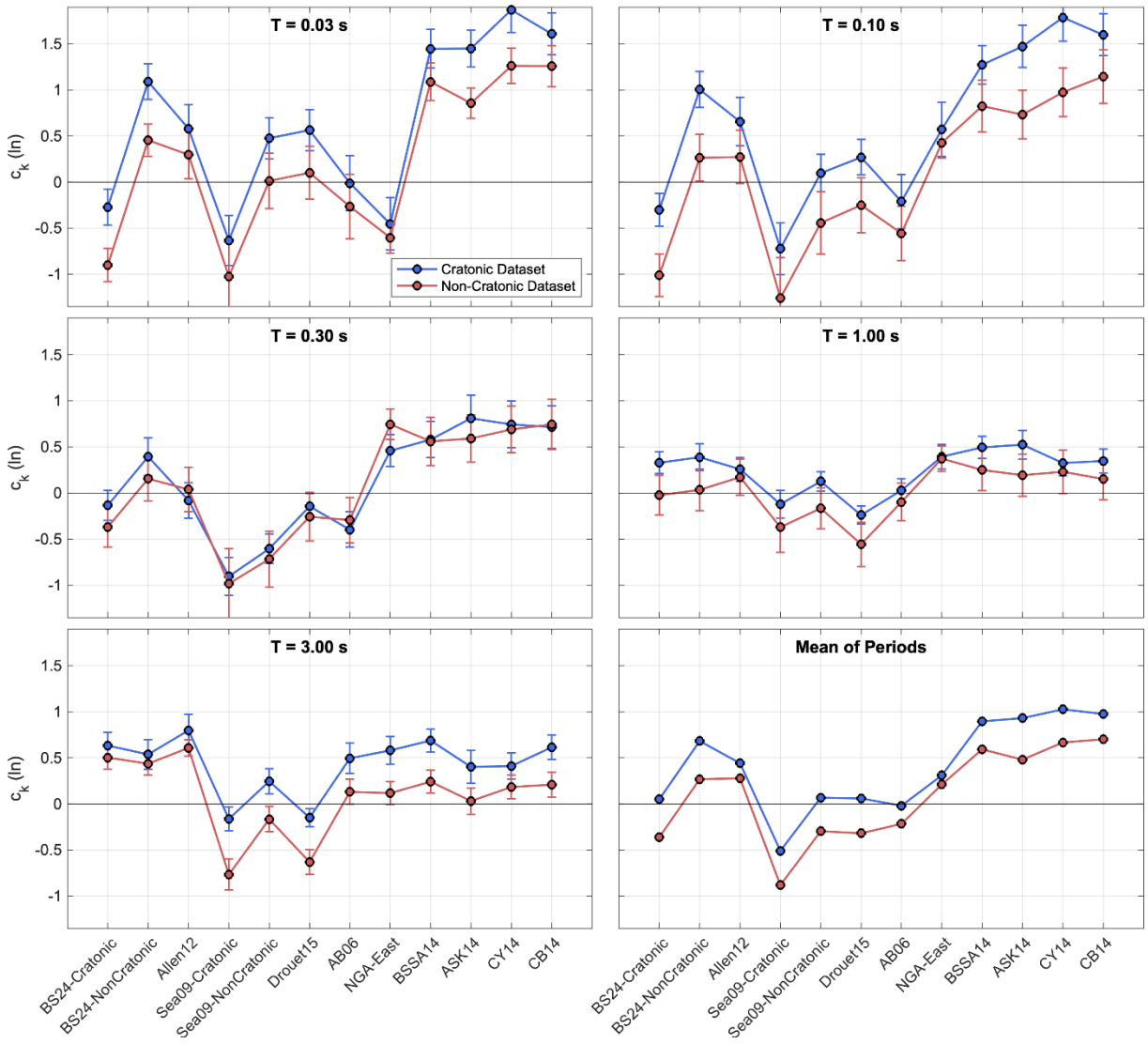

Figure 6. The GMM mean bias, c_k, for cratonic (blue) and non-cratonic (red) datasets and for five spectral periods. The sixth panel shows the mean of c_k across the five spectral periods.

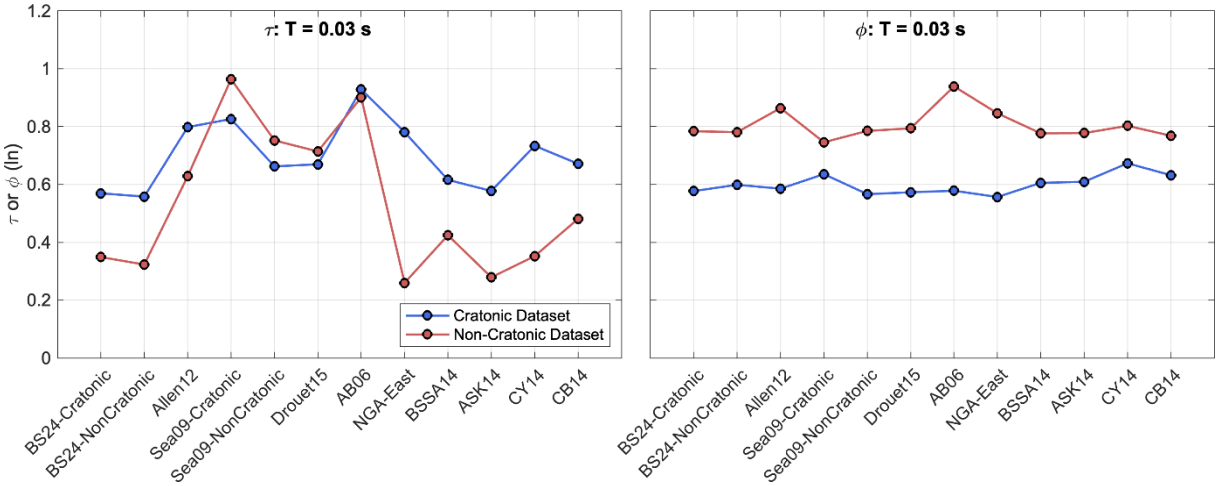

Figure 7. The values of τ and ϕ by GMM for cratonic (blue) and non-cratonic (red) datasets, T = 0.03 sec.

4 Stress Drop

Allen (2025) analysed stress drops for over 290 earthquakes in Australia in the magnitude range of 3.1 to 6.6. He identified significant regional variability in earthquake source characteristics for different seismotectonic regions, with earthquakes in Australia's northwest and Flinders Ranges regions having stress drops consistently higher than the median value in other areas. Allen (2025) found that the stress drop values appear to be approximately log-normally distributed, with a geometric-mean value near 1.9 MPa. We investigated whether there is a systematic difference in stress drops between the NSHA23 cratonic regions (including the Archaean and Non-Reactivated Proterozoic craton and Reactivated Proterozoic craton) and the NSHA23 non-cratonic region (Eastern Australian Phanerozoic Accretionary Terranes) using the stress drops from Allen (2025). Excluding earthquakes with hypocentral depth less than 3 km and earthquakes with stress drops less than 0.33 MPa, we found that the average stress drops for the cratonic and non-cratonic regions are 2.6 and 1.9 MPa, respectively, a difference of a factor of 1.4. Figure 8 shows a map of the NSHA23 tectonic regions and the Allen (2025) the stress drops from the earthquakes we used for this analysis. Most of the earthquakes in the Yilgarn craton have depths < 3 km, and we know that very shallow earthquakes in the cratons have special source (lower stress drop at shallow depth) and wave propagation characteristics (Lg wave generation). We are interested in comparing events without those known causes of differences in ground motions, to see if there are other factors such as static stress drop or crustal structure that might cause basic differences apart from the known ones.

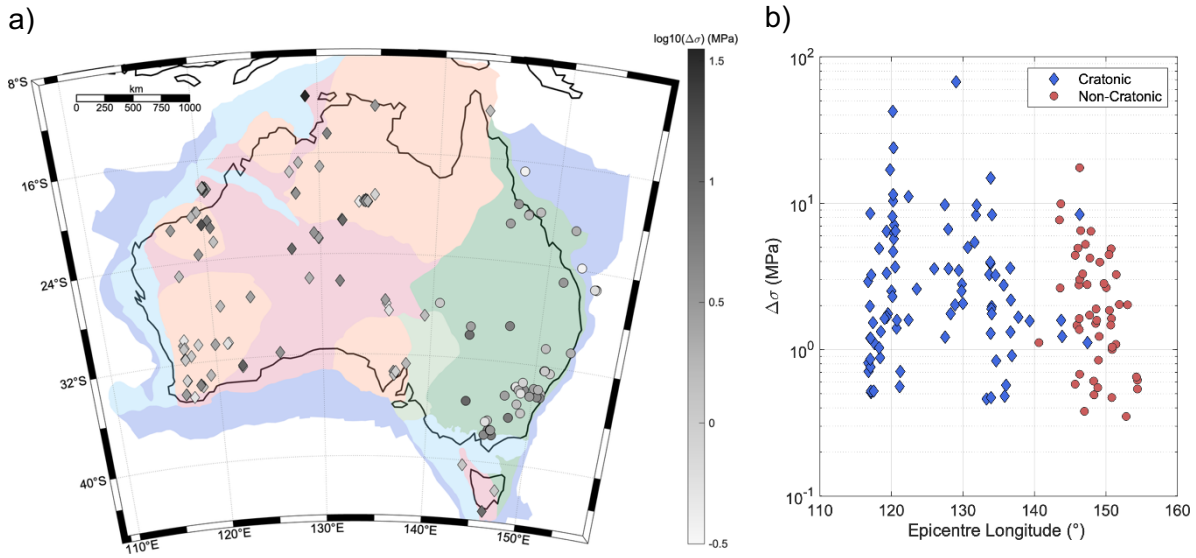

Figure 8. a) A map of Australia showing the NSHA23 tectonic regions (shaded colours; see also Figure 1) and the Allen (2025) stress drops used in the analysis (grayscale symbols), where diamonds are events from cratonic regions and circles are non-cratonic. b) The Allen (2025) stress drops analysed versus epicentre longitude.

The factor of 1.4 is smaller than but consistent with the difference in fault rupture area scaling between tectonically stable and active regions found by Leonard (2010, 2014), and the difference in stress drops obtained by Somerville (2021) and Allman and Shearer (2009). These differences are 6.5 vs 2.5 MPa, corresponding to a difference of a factor of 2 in rupture area in Somerville (2024); and 6.0 vs 3.0 MPa, corresponding to a difference of a factor of 2 in stress drop in Allman and Shearer (2009).

These differences in source dimension scaling are embodied in the ground motion simulations used in our BS24 GMM (Bayless and Somerville, 2024). They have a muted effect on the differences in simulated ground motions, because the effect of the larger fault displacement

averaged over a smaller rupture area in the cratonic fault models is partly offset because the displacement occurs over a longer rise time. The contrast in fault rupture area between the two regions also impacts probabilistic seismic hazard calculations. However, the main cause of differences between the cratonic and non-cratonic models is due to the differences in shallow crustal structure and in the high frequency stress parameter, which is distinct from the static stress drop as embodied in the relation between fault rupture area and magnitude.

We performed a two-sample t-test to test whether the unknown population means of the two groups (cratonic and non-cratonic stress drops) are significantly different or are different just due to random variation. In this test, the null hypothesis is that the two groups come from normal distributions with equal means, and the alternative hypothesis is that the means are not equal. The test was performed using the natural logarithm of the stress drops because they are approximately log-normally distributed as shown by Allen (2025). With a test statistic value of 1.96 and a t-value of 1.29, the null hypothesis was rejected at the 10% significance level (p = 0.05), in favour of the alternative hypothesis.

5 Magnitude and Distance Scaling

Probabilistic seismic hazard ground motions in Australia with long average return periods (e.g. 10,000 years; ANCOLD, 2019) are mostly dominated by moderate-magnitude earthquakes at near source distances, and depending on the location, can be significantly influenced by large magnitude (**M** 6.0 ~ 7.5) earthquakes at distances of 20 km or less (Somerville, 2016). The strong ground motions recorded from earthquakes in Australia are for magnitudes no larger than **M** 6, so it is important to use GMM's that reliably estimate the ground motions from larger magnitudes and near source distances. Globally, there are no data-based GMM's available for large earthquakes in stable continental regions, because of the paucity of strong motion recordings in other stable continental regions of the world. Instead simulation-based approaches have traditionally been applied.

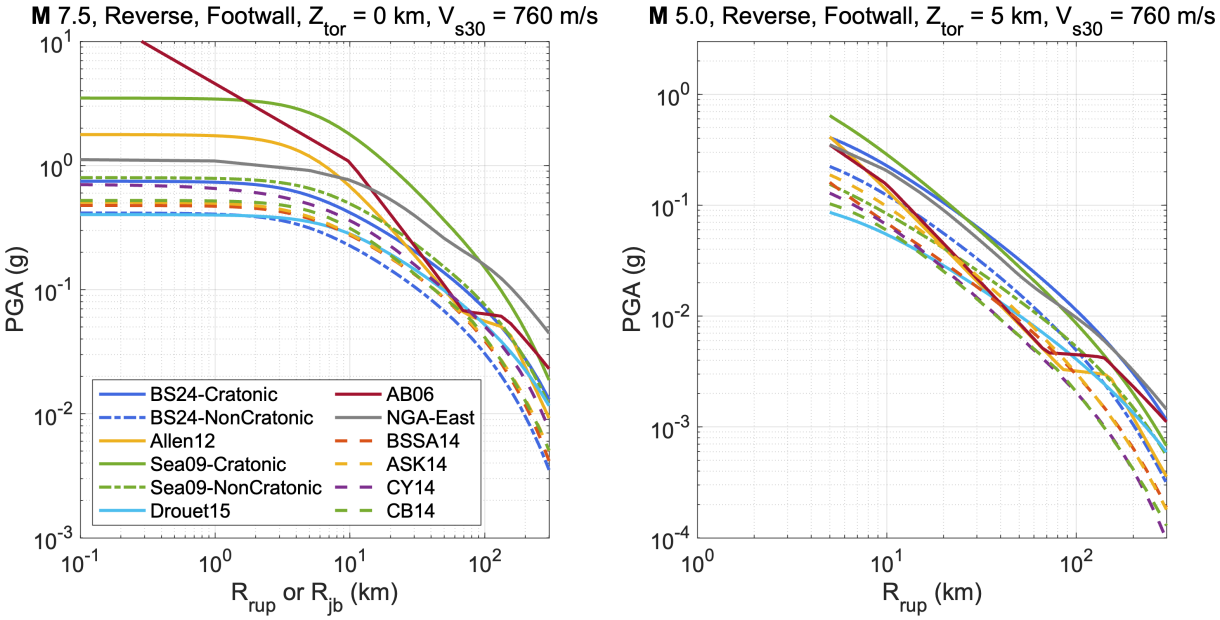

Figure 9. Comparison of the PGA distance scaling for twelve median GMMs and two scenario earthquakes.

Because empirical approaches are not possible for evaluating the GMMs in these critical magnitude and distance ranges, we compared the median GMMs of Table 1 for scenario earthquakes. Figure 9 compares the peak ground acceleration (PGA) distance scaling of the median GMMs for two scenarios. The first is a **M** 7.5 reverse faulting earthquake with Z_{tor} = 0

km, and all sites are assumed to be located on the footwall side of the rupture with V_{S30} = 760 m/s. The distance metrics R_{rup} and R_{jb} are equivalent for this scenario. The most striking feature of this figure is the AB06 model which predicts median PGAs larger than 10g for very small distances (median PGA = 4g at 1 km), representing extrapolation of the model to smaller distances than intended by the authors. Care must be taken when using this model with the full range of magnitudes and distances encountered in PSHA. This figure also shows that the Sea09-Cratonic median model predicts high PGAs for this scenario; higher than all other models besides AB06 for distances up to 100 km. Figure 9 shows that all models except AB06 model the magnitude-dependent effects of extended (finite dimension) ruptures on the distance scaling; resulting in less scaling at small source-site distances than at large source-site distances (Chiou and Youngs, 2008).

The second scenario in Figure 9 is a **M** 5.0 reverse faulting earthquake with Z_{tor} = 5 km, again with all sites assumed to be located on the footwall side of the rupture with V_{S30} = 760 m/s. For this scenario, R_{rup} values were converted to R_{jb} using the earthquake depth. For this smaller magnitude scenario, the four NGA-West2 models have short-distance scaling that is generally compatible with the other models, and have lower median PGAs than all models but Drouet15.

At larger distances, the distance-scaling of PGA for the four NGA-West2 models in Figure 9 are broadly similar to the BS24 and Sea09-NonCratonic GMMs for the **M** 7.5 scenario. The NGA-West2 models and BS24 attenuate more rapidly with distance than other models for the **M** 5.0 scenario. Relative to the NGA-West2 models, the NGA-East model has flatter PGA distance attenuaton at large distances because it is a model for tectonically stable regions, which are usually described by weaker effective anelastic attenuation than tectonically active regions (Baqer and Mitchell, 1998).

Figure 10 compares the magnitude scaling of the median GMMs at 80 km rupture distance for T = 0.01 sec (left) and T = 1 sec (right). At T=1 sec, the differences between models are relatively small. The Sea09-Cratonic model has strong magnitude scaling for **M** larger than about 7.0, which was an improvement addressed in BS24. At T = 0.01 sec, the BS24-Cratonic, Sea09-Cratonic, and NGA-East models have the highest ground motions for all magnitudes. The Sea09-Cratonic model is also an outlier at this spectral period in magnitude scaling for **M** < 5 and **M** > 7. The suite of four NGA-West2 models have large-magnitude scaling consistent with AB06, Allen12, BS24, Drouet15, and Sea09-NonCratonic. However, for **M** less than about 5.5, the four NGA-West2 models have very strong magnitude scaling at short periods (weaker ground motions for smaller magnitudes) relative to the other models. This, combined with the strong attenuation at large distances (Figure 9) is the primary cause of the short-period under-prediction on average of the Australian data by the NGA-West2 models.

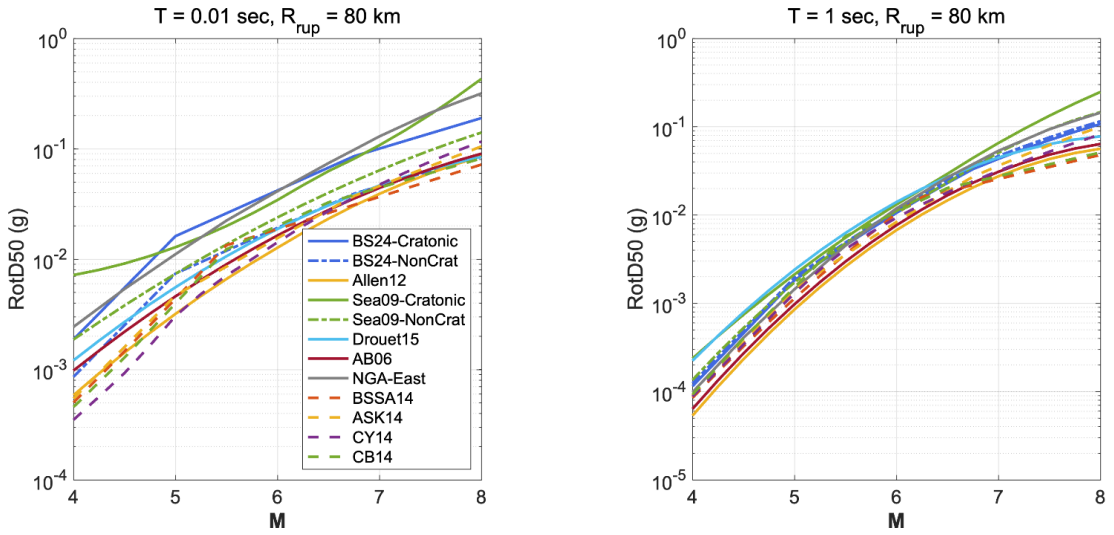

Figure 10. Comparison of the magnitude scaling for twelve median GMMs at 80 km distance, T = 0.01 sec (left) and T = 1 sec (right).

6 Distinctions Between Cratonic and Non-Cratonic Regions

The differences in shallow crustal earthquake ground motions between tectonically active and stable regions of North America are clearly defined in the NGA-West2 and NGA-East models, because the former are associated with plate boundaries. That is not the case in Australia, where we seek to understand potential differences between cratonic and non-cratonic regions that are distant from plate boundaries. In Australia, the non-cratonic regions include the Otway Ranges, Snowy Mountains, and Strzelecki Ranges, which experienced mountain-building uplift in the Cretaceous (145 to 66 million years ago; Müller et al., 2016). (This also occurred in the Flinders Ranges and Mt Lofty Ranges during the Sprigg Orogen, which we have excluded from the cratonic and non-cratonic regions used in the stress drop analysis).

In Western Europe, Weatherill and Cotton (2020) and Weatherill et al (2024, Figure 5) distinguish between northeastern Europe (the Baltic Sea and surrounding countries), which is a stable cratonic region characterised by an older, colder and thicker continental crust, and the rest of Europe; the transition broadly extends from Denmark to the north coast of the Black Sea. Weatherill et al. (2024) state that for the tectonically stable non-cratonic regions of northern and western Europe, they now give low weights to GMMs from stable cratonic regions that represent higher stress drop and slower ground motion attenuation. Similarly, NSHA23 (Allen et al., 2023; 2024) gave a weight of only 10% to the NGA-East ground motion model for use in non-cratonic Australia.

7 Conclusions

The first question posed in this study is if ground motions from non-cratonic earthquakes differ from those of cratonic earthquakes in Australia. With our GMM residual analyses, we found approximately 10% – 50% higher ground motions on average for the cratonic dataset. This difference was more pronounced at short and long spectral periods (T = 0.03, 0.1, and 3 sec). At intermediate spectral periods (T = 0.3 and 1 sec), the difference between regions was smaller and may not be statistically significant. Additionally, using stress drops from Allen (2025) we found that the average stress drops for the cratonic and non-cratonic regions are 2.6 and 1.9 MPa, respectively, a difference of a factor of 1.4.

The second question posed in this study is how applicable the NGA-West2 and NGA-East GMMs are to Australia. In our GMM residual analysis (Section 3), the four NGA-West2 median GMMs significantly under-estimate the short period Australian ground motions on average. This bias reduces with increasing spectral period. As shown in the bottom right panel of Figure 6, the average bias from the cratonic earthquake dataset of the two Australian models (BS24-Cratonic and Allen12) is about 0.25, similar to the bias of 0.3 for NGA-East, suggesting that it may be appropriate to use NGA-East in the cratonic regions of Australia. The average bias from the non-cratonic dataset of the two Australian models (BS24-NonCratonic and Allen12) is about 0.25, less than the average bias of 0.6 for the four NGA-West 2 models, suggesting that it may be appropriate to use the NGA-West2 models in the non-cratonic regions of Australia, although they may underpredict the ground motions at least for small earthquake magnitudes.

The above conclusions are subject to the limitations of the data, including uncertainties in site parameters (V_{S30} values and site amplification), uncertainties in source metadata (moment magnitudes, depths, and locations), and the overall limited quantity of data.

As noted in NSHA23 (Allen et al., 2023; 2024), empirical evaluations of the GMM performance only apply within the distance and magnitude ranges of the available dataset; in this case for small to moderate magnitudes, and such evaluations are not a reliable indication of performance in predicting larger events. For this reason, we compared the GMMs for larger magnitudes and shorter distance that are often critical to seismic hazard in Figures 8 and 9. The large-magnitude scaling of the NGA models are constrained by global earthquake data (NGA-West2) and by finite-fault earthquake simulations (NGA-West2 and NGA-East).

Both NGA projects were large, highly interactive, multidisciplinary research programs consisting of global experts. The technical issues addressed in these projects included the large magnitude scaling at close distances, hanging wall effects, style of faulting effects, and site and basin effects, among others, for the median and standard deviation of ground motions (Bozorgnia et al., 2014). Because of the great care that went into these models to capture the scaling of ground motions, particularly in magnitude and distance ranges where we do not have data in Australia, we consider these models applicable to Australia.

8 Acknowledgements

The authors thank Trevor Allen and Hadi Ghasemi at Geoscience Australia for making the cratonic region ground motion and source data publicly available and for providing the non-cratonic region response spectra, Andreas Skarlatoudis for reviewing the draft versions of the paper, and Trevor Allen and one anonymous reviewer for their helpful paper reviews.

9 References

Abrahamson, N. A., W. J. Silva, and R. Kamai (2014). Summary of the ASK14 ground motion relation for active crustal regions, Earthq. Spectra 30, 1025–1055, doi: 10.1193/070913EQS198M

Al Atik, L., N. A. Abrahamson, F. Cotton, F. Scherbaum, J. J. Bommer, and N. Kuehn (2010). The variability of ground-motion prediction models and its components, Seismol. Res. Lett. 81, no. 5, 794–801.

Al Atik, L. (2015). NGA-East: Ground-Motion Standard Deviation Models for Central and Eastern North America. PEER Report 2015/07. Pacific Earthquake Engineering Center, University of California, Berkeley.

Allen, T. I. (2012). Stochastic ground-motion prediction equations for southeastern Australian earthquakes using updated source and attenuation parameters, Geoscience Australia Record 2012/69, Canberra, pp 55.

Allen, T. I. (2025), Systematic Estimation of Earthquake Source Parameters for Continental Australia: Attenuation and Stress Drop. *Bulletin of the Seismological Society of America* 2025; doi: https://doi.org/10.1785/0120250054

Allen, T. I., Griffin, J. D. Clark, D. J., Cummins, P. R., Ghasemi, H., Ebrahimi, R. (2023). The 2023 National Seismic Hazard Assessment for Australia: model overview. Record 2023/53. Geoscience Australia, Canberra. https://dx.doi.org/10.26186/148969.

Allen, T. I., J. D. Griffin, D. J. Clark, and T. R. King (2024). The 2023 National Seismic Hazard Assessment for Australia: model input and output data, Geoscience Australia Record 2024/10, pp 81, doi:10.26186/149177.

Allmann, B.P. and P.M. Shearer (2009) Global variations of stress drop for moderate to large earthquakes. Journal of Geophysical Research 114: B01310.

ANCOLD (2019). Guidelines for design of dams and appurtenant structures for earthquake.

Atkinson, G. M., and D. M. Boore (2006). Earthquake ground-motion prediction equations for eastern North America, Bull. Seismol. Soc. Am. 96, 2181-2205, doi: 10.1785/0120050245.

Baqer S and Mitchell BJ (1998) Regional variation of Lg Coda Q in the continental United States and its relation to crustal structure and evolution. Pure and Applied Geophysics 153: 613–638.

Bayless J. and P. Somerville (2024). An Updated Ground Motion Model for Australia Developed Using Broadband Ground Motion Simulations. Proc. of the 2024 Australian Earthquake Engineering Society National Conference. 21-23 November 2024, Adelaide, South Australia.

Boore, D. M., J. P. Stewart, E. Seyhan, and G. M. Atkinson (2014). NGA-West 2 equations for predicting PGA, PGV, and 5%-damped PSA for shallow crustal earthquakes, Earthq. Spectra 30, 1057-1085, doi: 10.1193/070113EQS184M.

Bozorgnia Y, Abrahamson NA, Atik LA, et al. NGA-West2 Research Project. Earthquake Spectra. 2014;30(3):973-987. doi:10.1193/072113EQS209M

Campbell, K. W., and Y. Bozorgnia (2014). NGA-West2 ground motion model for the average horizontal components of PGA, PGV, and 5% damped linear acceleration response spectra, Earthq. Spectra 30, 1087-1115, doi: 10.1193/062913EQS175M.

Chiou, B. S.-J., and Youngs, R. R., (2008). An NGA model for the average horizontal component of peak ground motion and response spectra, Earthquake Spectra 24, 173–215.

Chiou, B. S.-J., and R. R. Youngs (2014). Update of the Chiou and Youngs NGA model for the average horizontal component of peak ground motion and response spectra, Earthq. Spectra 30, 1117–1153, doi: 10.1193/072813EQS219M.

Clark, D., A. McPherson, and R. Van Dissen (2012). Long-term behaviour of Australian stable continental region (SCR) faults, Tectonophys. 566-567, 1-30, doi: 10.1016/j.tecto.2012.07.004.

Drouet S, Cotton F (2015) Regional stochastic GMPEs in low-seismicity areas: scaling and aleatory variability analysis—application to the French Alps. Bull Seismol Soc Am 105(4):1883–1902

Ghasemi, H., and T. Allen (2021). Engineering ground-motion database for western and central Australia, Australian Earthquake Engineering Society 2021 Virtual Conference.

Ghasemi, H., and T. Allen (2023). Ground-motion database for southeastern Australia, Canadian Conference - Pacific Conference on Earthquake Engineering 2023, Vancouver, British Columbia.

Goulet, C.A, Bozorgnia, Y., Kuehn, N., Al Atik, L., Youngs, R.R., Graves, R.W. and Atkinson G.M. (2021). NGA-East Ground-Motion Characterization Model Part I: Summary of Products and Model Development. Earthquake Spectra, 37(S1): 1231–1282. https://doi.org/10.1177/87552930211018723

Gregor, Nick, Norman A. Abrahamson, Gail M. Atkinson, David M. Boore, Yousef Bozorgnia, Kenneth W. Campbell, Brian S.-J. Chiou, I. M. Idriss, Ronnie Kamai, Emel Seyhan, Walter Silva, Jonathan P. Stewart and Robert Youngs. (2014). Comparison of NGA-West2 GMPEs, Earthquake Spectra 30, 1179-1197.

Hashash, Y. M., O. Ilhan, J. A. Harmon, G. A. Parker, J. P. Stewart, E. M. Rathje, K. W. Campbell, and W. J. Silva (2020). Nonlinear site amplification model for ergodic seismic hazard analysis in Central and Eastern North America, Earthq. Spectra 36, 69-86, doi: 10.1177/8755293019878193.

Leonard M. (2010) Earthquake Fault Scaling: Self-consistent relating of rupture length, width, average displacement, and moment release. Bulletin of the Seismological Society of America 100(5A): 1971–1988.

Leonard, M. (2014); Self-Consistent Earthquake Fault-Scaling Relations: Update and Extension to Stable Continental Strike-Slip Faults. *Bulletin of the Seismological Society of America* 2014;; 104 (6): 2953–2965. doi: https://doi.org/10.1785/0120140087

Müller, R. Dietmar and Flament, Nicolas, el al. (2016). Formation of Australian continental margin highlands driven by plate–mantle interaction; Earth and Planetary Science Letters; Vol. 441; 60-70; 10.1016/j.epsl.2016.02.025

Seyhan, E., and J. P. Stewart (2014). Semi-empirical nonlinear site amplification from NGA-West 2 data and simulations, Earthq. Spectra 30, 1241–1256, doi: 10.1193/063013EQS181M.

Somerville, P. (2016). Seismic Hazard Assessment Methods including Deterministic and Probabilistic Methods and their uses in Dam Design. Proceedings of the 2016 Annual Conference of the Australian National Committee on Large Dams, Adelaide, 17-19 October.

Somerville, P.G., R.W. Graves, N.F. Collins, S.G. Song, S. Ni and P. Cummins (2009). Source and ground motion models of Australian earthquakes. Proceedings of the 2009 Annual Conference of the Australian Earthquake Engineering Society, Newcastle, December 11-13.

Somerville, P. (2021). Scaling relations between seismic moment and rupture area of earthquakes in stable continental regions. Earthquake Spectra doi: 10.1177/8755293020988024

Stewart, J. P., G. A. Parker, G. M. Atkinson, D. M. Boore, Y. M. A. Hashash, and W. J. Silva (2020). Ergodic site amplification model for central and eastern North America, Earthq. Spectra 36, 42-68, doi: 10.1177/8755293019878185.

Weatherill, G. and Cotton, F.: A ground motion logic tree for seismic hazard analysis in the stable cratonic region of Europe: regionalisation, model selection and development of a scaled backbone approach, B. Earthq. Eng., 18, 6119–6148, https://doi.org/10.1007/s10518-020-00940-x, 2020.

Weatherill, G. and Kotha, S. R. and Danciu, L. and Vilanova, S. and Cotton, F. (2024). Modelling seismic ground motion and its uncertainty in different tectonic contexts: challenges and application to the 2020 European Seismic Hazard Model (ESHM20), Natural Hazards and Earth System Sciences, 24, 5, 1795-1834. https://nhess.copernicus.org/articles/24/1795/2024/, doi: 10.5194/nhess-24-1795-2024.